Int J Adv Manuf Technol (2017) 93:1999–2011
DOI 10.1007/s00170-017-0601-x

ORIGINAL ARTICLE

Effects of hybrid electrical discharge machining processes on surface integrity and residual stresses of Ti-6Al-4V titanium alloy

Behnam Khosrozadeh[1] · **Mohammadreza Shabgard**[1]

Received: 6 January 2017 / Accepted: 1 June 2017 / Published online: 24 June 2017

Abstract The performance of the produced parts in the electrical discharge machining (EDM) is strongly influenced by the final quality of surface. High thermal gradients in EDM process develop considerable changes in surface integrity of machined samples such as changing the chemical composition of the surface, micro cracks appearance, recast layer, residual stresses, and reduction in fatigue life and corrosion resistance. Ultrasonic-assisted EDM (USEDM) and powder-mixed dielectric EDM (PMEDM) are two techniques in improving EDM efficiency. This paper was an attempt to investigate the effects of USEDM, PMEDM, and powder-mixed dielectric USEDM (PM-USEDM) processes on main characteristics of the surface integrity such as surface roughness, micro cracks, heat-altered metal zone, and residual stress. Scanning electron microscopy (SEM) micrographs were used to analysis micro cracks and heat-altered metal zone, and nanoindentation method was utilized to measure the amount of residual stress of discharged surface. The results indicated that PMEDM process improved surface roughness as well, induced micro cracks in PM-USEDM were very low, and heat-altered metal layer was very thick in traditional EDM comparing to PM-USEDM process which was thinner. The results of the present study also confirmed that the amount of residual stress of ultrasonic-assisted process was partially in lower level and had different profile compared with traditional EDM and PMEDM process.

✉ Behnam Khosrozadeh
behnam_kh@tabrizu.ac.ir

[1] Department of Mechanical Engineering, University of Tabriz, Tabriz, Iran

Keywords EDM · PMEDM · USEDM · Residual stress · Surface integrity

1 Introduction

Electric discharge machining (EDM) is an effective manufacturing process that provides hard materials machining with intricate shape which are different from those produced by the traditional machining processes [1]. In EDM, the electrical sparks are utilized for machining of electrical conductive materials. When distance between the electrodes is very little, the dielectric in this area is ionized and electric current can flow between electrodes which results in the happening of spark discharges that make plasma channel [2]. The spark energy develops very high temperatures (about 8000–12,000 °C) that are enough to melt and vaporize workpiece material [3]. At the end of pulse duration, the discharges terminates, some of the molten and vaporized materials are ejected from the workpiece and are removed by dielectric flow. The dielectric fluid limits plasma channel to a very small zone; hence, the intensity of plasma energy flux remains very high over a small area of the workpiece, and also this fluid carries away machining debris that are collected in the plasma gap between the tool and the workpiece [2]. The plasma channel develops very high pressure (about 3 Kbar) in spark channel. This pressure retains the molten material in place. At the end of pulse duration, electrical discharges disconnect and the pressure field collapses. The sharp pressure drop throws the melted and vaporized material from the molten puddle. The particles that were expelled from the spark zone freeze instantly in contact with the cold dielectric; finally, dielectric flow takes away the produced debris [4].

Every spark creates a cavity on the workpiece surface and a smaller one on the tool electrode. In a single discharge, only a

small fraction, about 15% or less, is removed by the dielectric. The rest of the melted material resolidifies to form recast layer [5]. This layer, that is difficult to etch, is known as the white layer. Moreover, under the white layer, there is a layer in which intense heating and rapid cooling change its microstructure and mechanical properties. One of the characteristics of EDM process is the abundance of micro cracks on machined surface. These cracks are generated due to the thermal stresses and transformational changes happen in the workpiece body as the result of fast cooling after discharge, and it often reaches to the ultimate strengths of the material. The cracks usually penetrate into recast layer and cause the reduction of wear, fatigue, and corrosion resistance of EDMed specimens [5, 6]. Thermal processes, as well, develop residual stresses at machined surface. These stresses are generated due to high temperature gradients that were aroused from rapid thermal loads and thermal shrinkage of resolidified layer of machined workpiece, along with plastic deformation and phase transitions [7]. The residual stress affects the fatigue performance, dimensional accuracy, and stress corrosion resistance of a discharged component.

In order to decrease abovementioned limitations, EDM process has made use of techniques such as chemical processes, ultrasonic aided mechanisms, powder-mixed dielectrics, etc. Regarding residual stress of EDM process, Kremer et al. studied the effects of ultrasonic vibration on EDM performance. Their findings indicated that ultrasonic vibrations had considerably improved the EDM process; in this condition, residual stresses were less at a certain depth compared with pure EDM. However, there was no significant difference at surface residual stresses. Also, ultrasonic vibration had a positive effect on fatigue life and the reduction of affected layer [8]. Ekmekci et al. (2005) evaluated induced residual stresses in EDM process. They used layer removal technique for measuring residual stress along the depth of machined surface. The results showed that residual stresses along the depth increased to their maximum value which was approximately near the ultimate tensile strength of the material. Then, residual stress decreased quickly to comparatively low compressive stresses. The model of residual stress curve along the depth was the same at various pulse durations and currents except at samples which had cracking network. The depth of maximum residual stress was dependent on the discharge energy [9]. Guo et al. combined ultrasonic vibration and wire electrical discharge machining (WEDM). The outcomes indicated that applying vibrations generally promoted WEDM efficiency, so that material removal rate increased and the surface quality improved. The use of X-ray diffraction method revealed that residual stress in ultrasonic aided WEDM process was lower than WEDM process [10].

Mamalis et al. determined residual stress distribution of micro alloyed steel in EDM process by utilizing X-ray diffraction method. They found that there was significant amount of residual stresses at the inner layer. It was demonstrated that the maximum amount of stresses was approximately independent of the spark energy and reached the ultimate strength of the material. Increase in discharge energy entailed increase in the depth that the maximum residual stress happens, because of the presence of the excessive amount of surface cracking with high-energy discharges [10]. Das et al. (2003) simulated residual stresses and microstructure changes in EDM process by the use of finite element method and compared the results with experimental data. They reported that the amount of residual stress in a single discharge near the discharge location would reach to the tensile strength of the material. It might develop micro cracks in the heat affected zone. Induced residual stresses profile versus depth implied that these stresses had very high amount near the machined surface, but they vanished quickly in the inner layer region [11]. Guu et al. (2003) analyzed EDM-altered surface properties and machining defects of AISI D2 steel. They correlated residual stress and EDM inputs using regression modeling. The model revealed that pulse current had more effects on residual stress in comparison to pulse duration. Electrical discharge machining developed micro defects which were stress concentration sites, those that initiated cracks. This micro defects reduced the capacity of strain energy density and led to the reduction of the strength of material [12]. The amount of subsurface residual stress and microstructure changes of tool steel in EDM process had been evaluated by Ghanem et al. Residual stresses that were measured by XRD method revealed peak tensile stresses (close to ultimate strength of material) which was about 50 μm under the discharged location. Surface hardness of machined samples was almost four times of bulk material hardness. This change was depended on the change of near surface phase and carbon decomposition of hydrocarbon dielectric [13].

Ghanem et al. surveyed fatigue life of tool steel in finishing EDM process. The measurement of residual stresses indicated that the isotropic stresses mean peak value was 750 MPa at subsurface. Tensile residual stresses had changed to compressive mode at about 120 μm depth. They found that by removing EDM-induced surface cracks and applying compressive residual stresses, endurance limit of machined samples improved 70% compared with untreated samples [14]. Fatigue and fracture properties of EDMed WC-CO were studied by Casas et al. The results showed that the main cause of strength reduction was related to EDM-produced residual stresses. Posttreatment was required for electrical discharged specimens, which were subjected to fatigue loads in order to eliminate or reduce the residual stresses level [15]. Rebelo et al. (1998) considered the correlation between spark energy and surface integrity of martensitic steels in EDM process. The results of their experiments expressed that the depth of peak residual stress was related to the average depth of EDM cracks penetration. The appearance of the most of the cracks on surface and subsurface corresponded to the relief of stresses. For

this reason, spark energy influenced mainly the depth in which the largest amount of residual stress appeared; so, as the discharge energy increased, the affected depth increased, too. Therefore, induced residual stress diminished at surface as the result of the increase of the spark energy [16]. Yang et al. (2013) used molecular dynamics technique to simulate residual stress induced in EDM process. They reported that the amount of the stresses inside resolidified region meaningfully oscillated in sparking period. With the passing of time, the normal stresses at the specimen surface were changed from compressive stress to tensile one, and stresses in interior layers were left at compressive state. Therefore, tensile residual stresses existed in surface and close surface layers and compressive residual stresses remained at interior regions. This implied that the surface of machined parts by EDM process was prone to crack generation and growth [17].

Review of research literature revealed that there are few studies about EDM and residual stress induced in EDM process, especially in the case of EDM variables and their effects on residual stresses. Also, there is not any comprehensive work regarding hybrid EDM and surface integrity components, particularly residual stress, whereas surface integrity is a feature of the workpiece that is affected by hybrid EDM mechanisms. The main aim of this study was to investigate the machining characteristics of titanium alloy Ti-6Al-4V using EDM and hybrid EDM processes (applying ultrasonic vibration to tool electrode, adding nanopowder into dielectric in EDM and simultaneous utilization of ultrasonic vibration and addition of nanopowders). It is probable that ultrasonic vibration of tool in PMEDM process causes uniform distribution of the nanoparticles in dielectric medium and increases the nanoparticle energy in the presence of elastic waves, which improves nanopowders influence in EDM process. The hybrid EDM processes were performed in different machining settings (pulse duration and pulse current) to evaluate the machining efficiency, surface integrity, and residual stress.

2 Materials and method

2.1 Material

Ti-6Al-4V is one of the most widely used alloys because of its potential in maintaining excellent physical properties even at high temperatures. Some of the characteristics of these alloys include low weight associated with high strength, excellent resistance to fatigue and creep, good resistivity in corrosive environments, and biocompatibility. Ti-6Al-4V is used in various areas such as automotive, biomedical, aerospace, marine, and chemical processing industries. Due to the limitations of machining, this alloy (like low thermal conductivity and work hardening) with traditional machining, non-conventional machining methods, like laser beam machining, electrochemical methods, and EDM process was used for machining this type of material (chemical composition of this alloy is provided in Table 1). The utilized samples in this experiment were prepared from titanium bar by the use of wire cut machine. All of titanium bars were cut at a height of 10 mm with diameter of 14 mm. The surface of samples that were subjected to machining operation was polished with grinding machine. At the end of the sample preparation phase, before EDM experiments, the samples were placed at heat treatment furnaces for 2 h at 500 °C and then were cooled down slowly in the air to conduct stress relief treatment [18]. Tool electrodes were made of copper bar by the use of turning operation, and some of the electrodes that were attached to ultrasonic head were threaded. Table 2 illustrates the physical and mechanical properties of the titanium alloy and the copper electrode.

Table 1 Chemical composition of Ti-6Al-4V alloy in %

H	N	C	O	Fe	V	Al	Ti
0.0053	0.01	0.02	0.18	0.22	4.02	6.08	89.464

2.2 EDM and hybrid machining condition

EDM tests were performed with Charmilles Roboform 200 die sinking apparatus that had an Iso pulse generator. In order to control the process stability and compare the pulse shapes in different processes, an electronic circuit was connected to PC to display and record the voltage and current pulses. In hybrid machining mode, the tool electrode vibrated by ultrasonic frequency and SiO2 nanopowder was added to dielectric fluid. Because of applying ultrasonic vibrations to the tool electrode, an ultrasonic head with 20 kHz vibrating frequency and 200 W power mounted on EDM machine. Schematic setup of equipment used in the experiments is presented in Fig. 1. Machining experiments were performed according to the design of experiments (DOE) full factorial technique; accordingly, four levels were considered for current and pulse duration. Two kinds of dielectric (with and without nanopowder) were utilized, and all tests were conducted in two different modes of tool electrode (with and without ultrasonic vibration); all of the machining tests were repeated three

Table 2 Physical and mechanical properties of workpiece and tool materials

Material	Copper tool	Workpiece (Ti-6Al-4V)
Modulus of elasticity	110 Gpa	113 Gpa
Melting point	1084 °C	1660 °C
Density	8.9 g/cm3	4.43 g/cm3
Electrical resistivity	16.78 nΩ.cm	178 μΩ.cm
Thermal conductivity	401 W/m.K	6.7 W/m.K

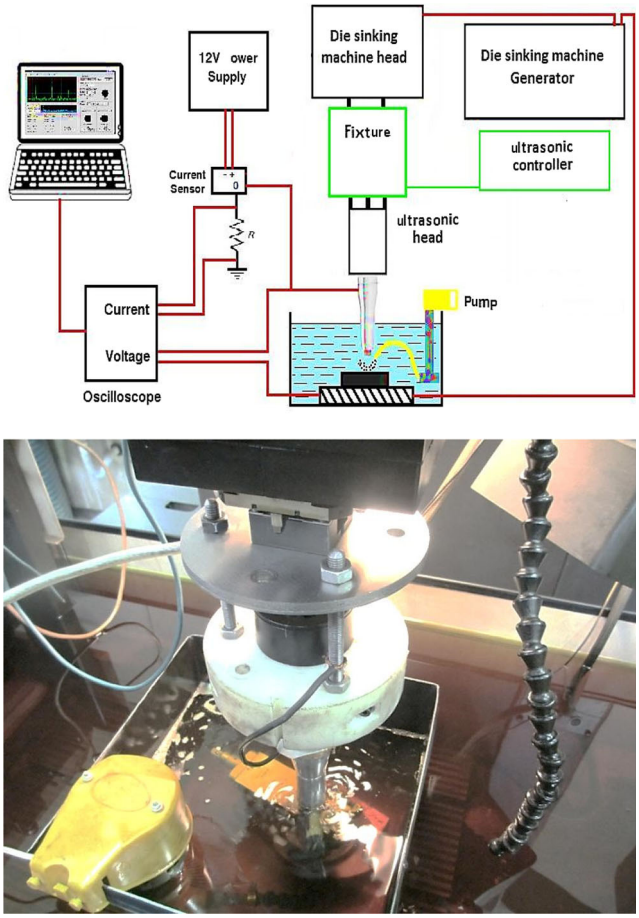

Fig. 1 Schematic setup and real picture of experiments

times; other parameters were constant. Table 3 indicated the other machining settings and experiments inputs.

2.3 Surface characterization

In order to study the surface morphology, the distribution of cracks and depth of heat-affected layers, the scanning electron microscope (SEM) instrument (MIRA3 FEG-SEM) was used. The samples were cut perpendicular to the machined surface by using wire EDM, and after polishing, they were etched by using Kroll's reagent. It was composed of 92 ml distilled water, 6 ml nitric acid, and 2 ml hydrofluoric acid; the samples were immersed in etching solution for 15 s [19]. Surface roughness of machined workpiece was measured by surface roughness measuring device (Mahr-Perthomether M2). The mean value of three measured data in different directions was regarded as surface roughness in Ra scale.

Table 3 Input variables and process parameters of spark

Input variable	Value
Pulse duration (μs)	400, 100, 25, 6.4
Pulse current (A)	48, 24, 12, 6
Pulse off time (μs)	6.4
Open circuit voltage (V)	200
Gap distance (μm)	50
Dielectric	Oil flux ELF

2.4 Residual stress measurement and methodology

There are many techniques for the measurement of residual stress in components. Some of them are destructive, some semi-destructive, and others are nondestructive methods. Most of these methods have limitations such as material type and its structure, depth of penetration, inaccuracy of strain measurement, the complexity of measurement, and expensiveness [20]. In comparison to these methods, the current study applied a procedure that was simple, less complex, and inexpensive to determine residual stresses. In this method, named as nanoindentation, microhardness test was used to determine the state of residual stress in material. This method was firstly introduced by Suresh and Giannakopoulos. Nanoindentation is based on the principle that the residual stress in the material influences indentation load depth curve, so by analyzing and comparing between stressed indentation curve and unstressed one, the amount of residual stress in intended region could be obtained. The differences in indentation deformation induced by residual stress were estimated in load depth curve (Fig. 2). In practice, various parameters influence this procedure. The most serious of these factors includes thermal drift (creep within the specimen material and change in dimensions of the instrument due to thermal expansion), surface roughness of workpiece, first contact of indenter with the specimen surface before the displacement measurements, instrument compliance, and indenter geometry. Others arise from environmental changes during the test, material-related issues such as crystallographic effects, friction state between the tip and material history (strain hardening or relief) [21].

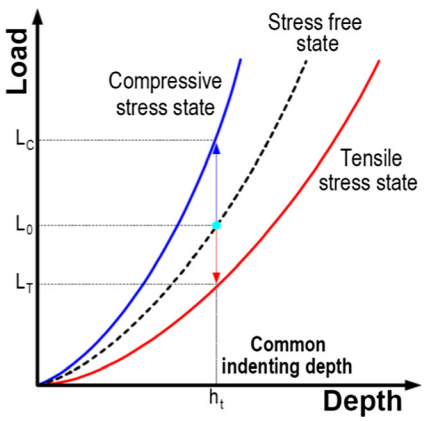

Fig. 2 Load depth curve in nanoindentation technique

In the indentation curve, applied force for specimens with compressive residual stress was higher in comparison to unstressed state. It was confirmed that loading curve had more slope than stress-free loading curve. Conversely, in specimens with tensile residual stress, applied force was less than unstressed state, and related loading curve had fewer slope than stress-free loading curve.

It was assumed that residual stress to be equi-biaxial plane stresses ($\sigma_{residual,x} = \sigma_{residual,y} = \sigma_{residual}$ and $\sigma_{residual,z} = 0$), this stress composed of hydrostatic stress ($\sigma^{Hydro} = \frac{2}{3}\sigma_{residual}$) and plastic deformation sensitive shear deviator stress ($\sigma^{Deviator} = \frac{1}{3}\sigma_{residual}$). The residual stress component in the direction of applied indentation force in the deviatory stress section was added to indentation pressure that was applied perpendicular to the surface [22]. Therefore, the variations between indentation forces in stressed and unstressed samples indented to a penetration depth, L_T–L_0, introduced as residual stress. The relationship between indentation load and equi-biaxial residual stress is presented in Eq. (1):

$$\sigma_{residual} = 3(L_0 - L_T) \Big/ \left(2A_C^T\right) \quad (1)$$

In Eq. (1), the real contact area between indenter and sample was shown by A_C^T.

In the current research, the amount of residual stress had been measured by calculating the variations between indented contact areas of unstressed and stressed specimens utilizing the analysis of loading curves according to the following equations [23]:

In tensile residual stress condition:

$$\sigma_r = H\left(1 - {}^{A_0}/_{A}\right) \quad (2)$$

In compressive residual stress condition:

$$\sigma_r = H\left(1 - {}^{A_0}/_{A}\right) \Big/ f \quad (3)$$

In these equations, A and A_0 were the indentation contact areas of stressed and unstressed samples. H was the hardness of material and the geometric factor of the indenter was presented by f. All the indentation experiments were load-controlled tests with 1000 mN applied force and Berkovitch indenter with 100 nm tip radius was used. Every indentation experiment was repeated three times and indentation curves of each machining process were plotted using mean value of obtained data.

3 Results and discussion

3.1 The effects of hybrid EDM processes on material removal rate

Material removal rate (MRR) was one of the most important outputs of EDM process. In rough machining conditions as the value of this parameter increases, the machining efficiency will exceed, too. In finishing conditions, mostly high magnitude of MRR affects adversely on the quality of produced surface. MRR (mm^3/min) is defined as follows:

$$MRR = (M_1 - M_2) \times 10^3 \Big/ (\rho_{Ti} \times t) \quad (4)$$

In Eq. (4), M_1 and M_2 are the workpiece mass (gr) before and after machining, respectively. ρ_{Ti} is the density of titanium alloy (gr/cm^3) and duration of machining is represented by t (min). One of the main reasons of hybrid or combined EDM processes is the increase of MRR. In this study, in order to study the effect of hybrid processes on MRR and other desired outputs, MRR ratio parameter was defined as follows:

$$\text{MRR ratio} = \text{MRR of hybrid EDM} \Big/ \text{MRR of traditional EDM}$$

The analysis of adding nanopowders and the application of ultrasonic vibration separately and simultaneously in EDM process on MRR can be carried out more easily by the use of MRR ratio. The results of different EDM processes versus pulse duration and current on MRR ratio are presented in Figs. 3 and 4, respectively. As it is apparent from these figures, MRR of hybrid processes is higher than the traditional EDM (MRR ratio >1). In this case, the effect of applying ultrasonic vibration on MRR ratio was more than the addition of nanopowders in dielectric, and the combination of these hybrid processes had the greatest influence on MRR ratio, too. The increase of MRR ratio by applying ultrasonic vibration of tool could be attributed to the following reasons:

1. Ultrasonic waves transport energy and momentum that are passed to the charged particles in discharge zone; this causes the production of acousto-electric current. The free charge modulation produced by acoustic wave increases collision ionization and brings about faster growth of streamers in the breakdown process of the dielectric [24]. The produced acousto-electric current I is introduced by Eq. (5)

$$I = {}^{\mu P_d}/_{LV} \quad (5)$$

In Eq. (3), μ and P_d are the movability of charged particles and acoustical power transferred to charged particles, respectively. The interplay span and the phase speed are introduced by L and V, respectively.

The produced agitation in dielectric would further improve deionization and remove any adhering particles from the electrode surface; hence, it results in decreased arcing and micro shorts relatively.

2. Ultrasonic vibration of tool increases charged particles energy inside discharge channel. The amount of the increase (δE_Z) can be explained by Eq. (6).

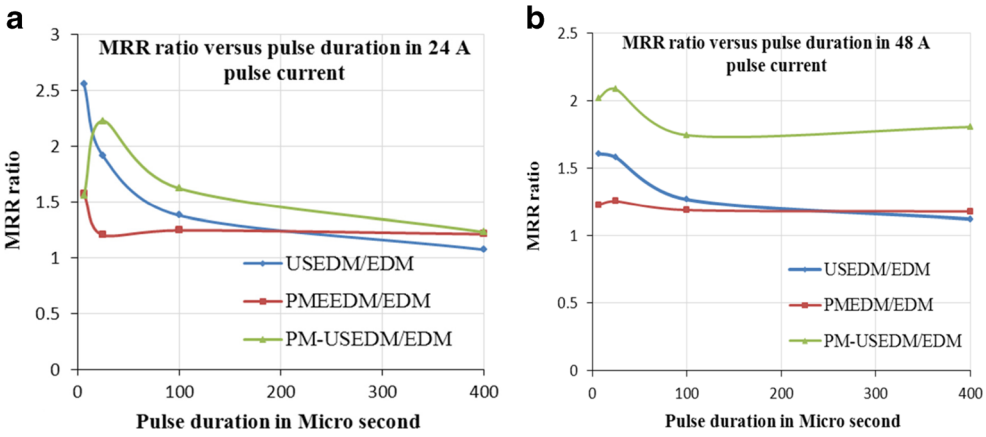

Fig. 3 The effect of hybrid EDM processes on MRR ratio versus pulse duration in **a** 24 A pulse current and **b** 48 A pulse current

$$\delta E_z = {}^{1}/_{t_p}\int_0^{\tau}\frac{1}{2}M_s u^2(t)dt = {}^{M_s U^2}/_{4} = M_s\pi^2 f^2 A^2 \qquad (6)$$

In Eq. (6), t_p, A, and M_S are the period of the vibration, amplitude of vibration, and mass of a plasma particle, respectively. The amplitude at any instant and the maximum amplitude of the vibration are presented by u and U [25].

3. When tool vibrates with ultrasonic frequency, compressive and refractive waves are produced; accordingly, micro bubbles and micro streams appear inside plasma channel. They act as a pump and removes debris and machining products from the gap efficiently. By renewal of dielectric fluid, short and open circuit pulses are reduced. Therefore, the stability of machining is improved.
4. Ultrasonic waves in expansion phase have the aggressive action in plasma channel and facilitate the ejection of melted material from the molten puddle; as well, in contraction phase, the pressure drop inside the plasma channel resulted in strong suction force inside the discharge region in which intense bulk boiling is developed and molten material is exploded away from discharge location. So, the amount of removed material from workpiece increases [26, 27].

The addition of nanopowders to dielectric did not have any significant influence on MRR ratio; however, in low-energy conditions (low-pulse current and low-pulse duration), this addition increased the amount of MRR ratio (Fig. 4a). In low-energy pulses, plasma channel energy was not sufficient to overcome the dielectric breakdown strength; in contrast, the addition of powder particles in dielectric reduced the breakdown strength of dielectric. Likewise, sparks could take place in lower pulse currents and durations which resulted in the increase of MRR ratio in this condition. The deduction of MRR ratio that was caused by the increase of pulse duration in Fig. 3a was due to the accumulation of machining debris in machining gap.

The application of nanopowders in dielectric and ultrasonic vibrations of tool simultaneously amplified the effects of each other. This would be as the results of two reasons: better dispersion of the nanoparticles in the presence of ultrasonic vibration and the increase of nanoparticles energy in the presence of acoustic waves in dielectric. In both cases, ionization of plasma channel had developed quickly. Also, using nanopowder, electrons and ions moving in the dielectric had been accelerated in the presence of ultrasonic vibrations and had been collided with nanopowder particles. These particles produced more electrons and ions by absorbing energy. This

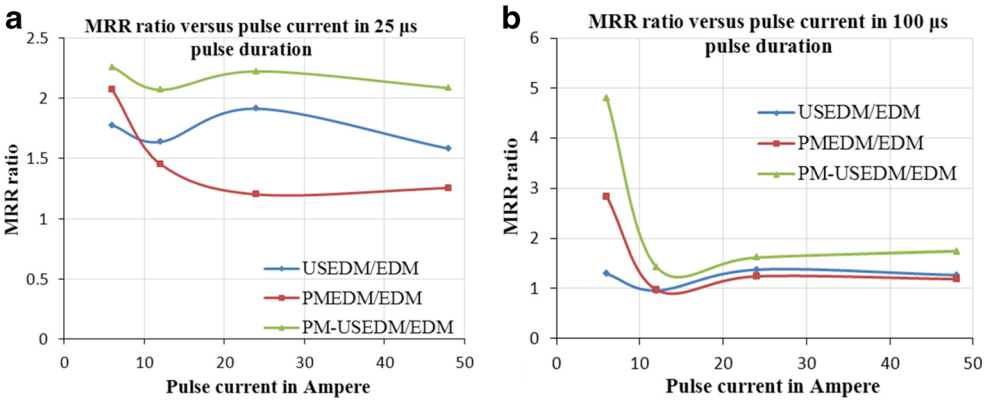

Fig. 4 The effect of hybrid EDM processes on MRR ratio versus pulse current in **a** 25-µs pulse duration and **b** 100-µs pulse duration

phenomenon increased the number of sparks per unit of time (spark frequency) [28, 29].

3.2 The effects of hybrid EDM processes on surface roughness

Figure 5a, b depicted the effects of hybrid EDM processes on the surface roughness versus pulse duration and pulse current. SEM micrographs of machined surface in different hybrid EDM processes are presented in Fig. 6. As it is apparent from these figures, the application of ultrasonic vibration increased surface roughness of machined specimens (Fig. 6c, d). The reasons of this could be demonstrated as follows: During the application of ultrasonic vibrations, as the result of better cleaning of discharge gap and increased energy of plasma particles, the energy of each discharge enhanced. Therefore, the amount of melted material and expelled out of the molten puddle increased in bulk boiling process. It resulted in enhancement of the depth of cavities after solidification. As a result, the surface roughness increased [30]. Ultrasonic vibration was also applied in PM-USEDM process, even though the effects of this vibration were further in the presence of nanoparticles. Because of applying vibration, the velocity and the acceleration of particles in the dielectric increased and collided with workpiece; the momentum of this movement threw out more molten material from the molten puddles. It increased both the depth of the holes and the surface roughness [29].

Considering the high speed and acceleration of tools due to ultrasonic vibrations, these movements acted like a pump and increased fluid movement in the gap; in the shortest time, the fresh dielectric was replaced by the polluted dielectric. These factors provided the conditions for eliminating arc and short circuit pulses and increasing the number of normal pulses. Normal and high-energy pulses created deep craters and enhanced surface roughness.

In both USEDM processes (with and without powder), the tool oscillated with 20 KHz frequency. In these methods, the cycle of upward movement of the tool developed pressure drop in machining gap, and much more molten materials were ejected from molten puddles compared with the traditional EDM; as a result, the depth of cavities and surface roughness were increased [30]. The lowest surface roughness among the mentioned processes belonged to PMEDM process (Fig. 6b). Improved surface finish was one of the most important features of adding powder in dielectric in EDM process. Adding nanoparticles in dielectric resulted in the enhancement of machining gap and spark frequency; in this condition, sparks energy and the electric field intensity distribution were more uniform. By reducing the high-energy sparks and electrostatic capacitance between the electrodes via distance increase, pulses with very low current and low energy led to the creation of smaller sparks and shallower cavities, as it is evident in SEM Fig. 6b. Accordingly, it was confirmed that surface finish would be improved along with increase in machining rate [31].

3.3 The effects of hybrid EDM processes on surface micro cracks

Surface micro cracks are considered as the important factors that influence surface integrity of produced parts. The number and the distribution of micro cracks have determinant role in the performance and fatigue resistance of machined samples. As well, regarding the fact that EDM is an electro thermal process; therefore, the development of surface micro cracks in machined components is inevitable. But controlling the size and the number of micro cracks by controlling discharge energy is possible. Figure 7 shows the produced cracks on machined surface in different hybrid EDM processes. According to Fig. 7, it is clear that traditional EDM process had

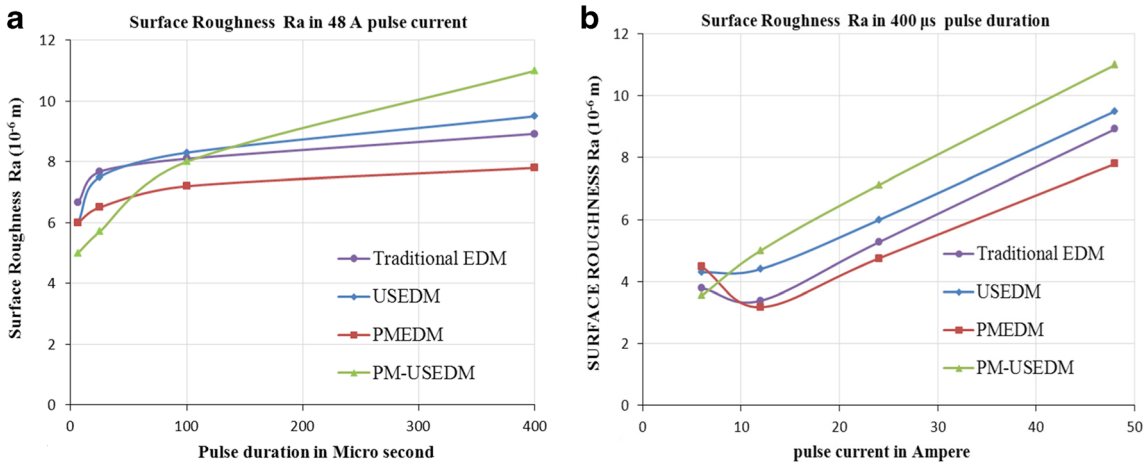

Fig. 5 The effect of hybrid EDM processes on surface roughness **a** versus pulse duration in 48 A pulse current and **b** versus pulse current in 400-µs pulse duration

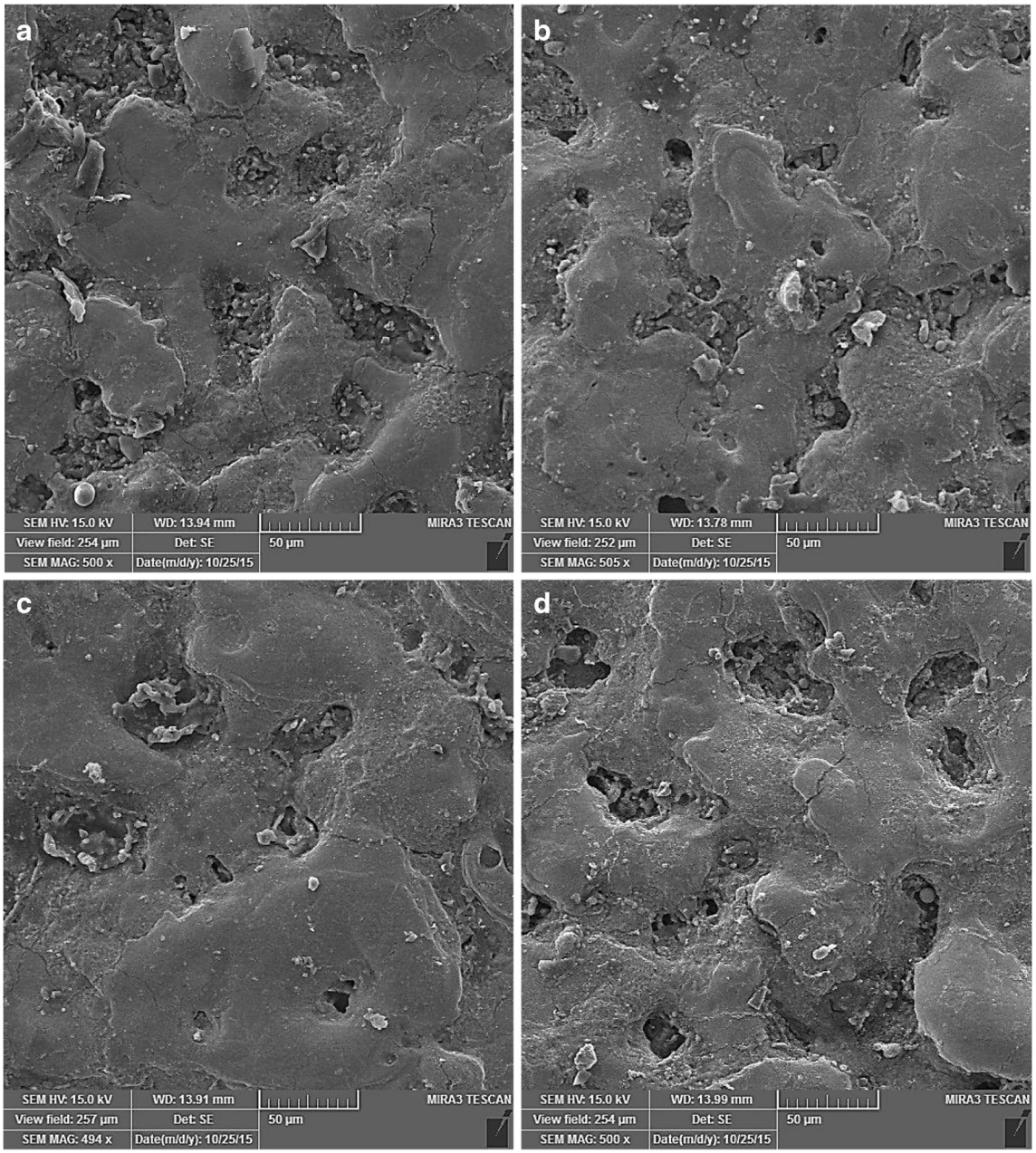

Fig. 6 SEM micrograph of produced surfaces in processes **a** EDM, **b** PMEDM, **c** USEDM, and **d** PM-USEDM, machining parameters: 48 A pulse current and 400-µs pulse duration

developed wider and greater cracks (Fig. 7a). In ultrasonic-assisted and nanopowder-mixed dielectric processes, Fig. 7b, c, the length and the width of cracks had been decreased. Regarding surface cracks, surface quality was very favorable in PM-USEDM process as shown in Fig. 7d.

In PMEDM, nanoparticles increased spark frequency and the large number of discharges with lower energy was generated in the discharge region. As well, nanopowders enlarged and widened the plasma channel. Consequently, the number of parallel sparks in machining zone was increased and electric energy was uniformly distributed among the sparks. In conclusion, transferred thermal energy to the workpiece was distributed in larger area and the input energy intensity was reduced per unit of area. With regard to the aforementioned reasons, thermal stresses and solidifying shrinkages were reduced which resulted in the deduction of the length and the width of produced cracks.

In the USEDM process, material removal rate was higher than the traditional EDM. This was because of the ultrasonic waves that left less volume of resolidified material on machined surface; hence, lower thermal stresses and fewer cracks appeared on the machined surface. In PM-USEDM process,

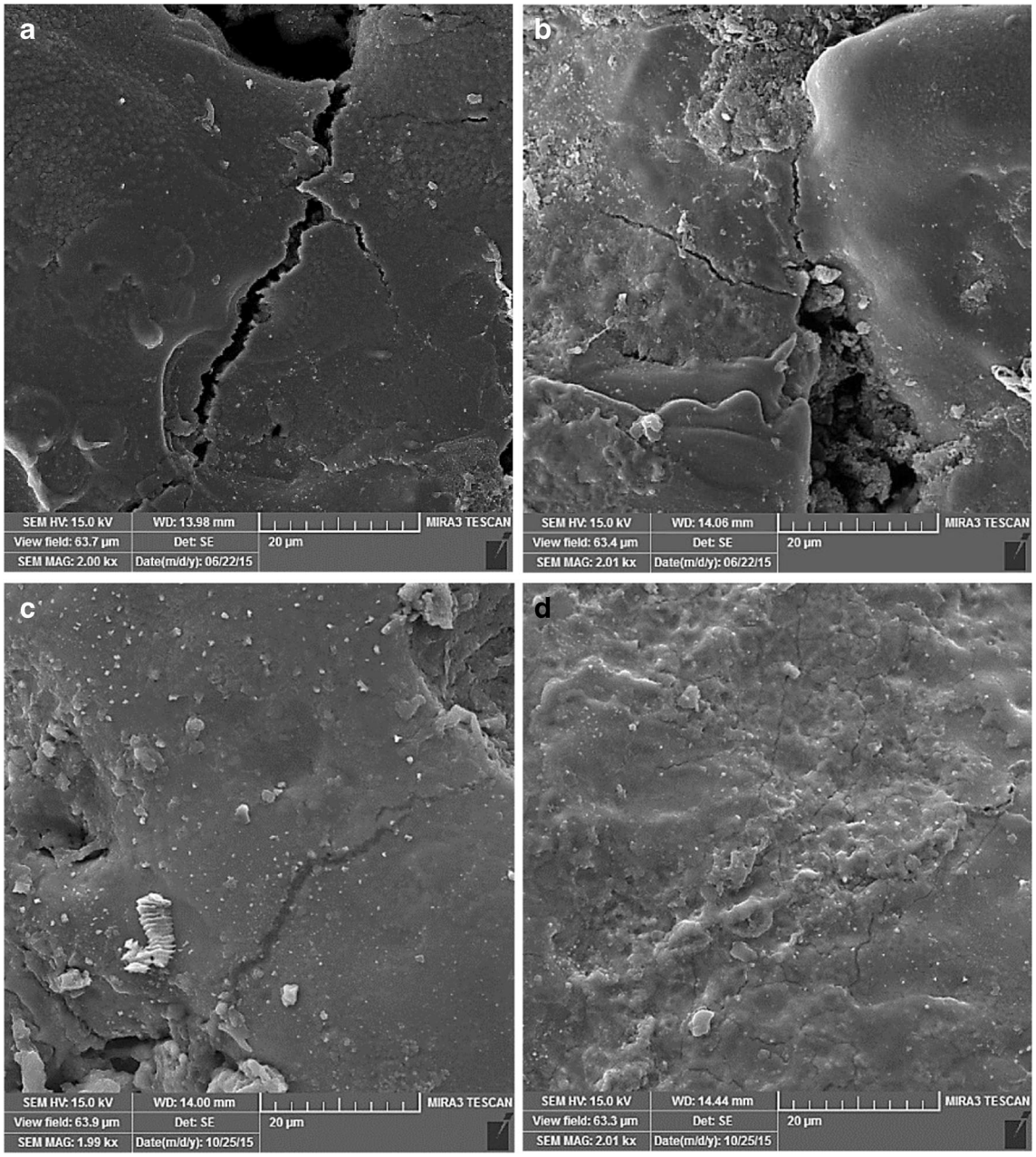

Fig. 7 SEM micrograph of surface micro cracks in processes **a** EDM, **b** PMEDM, **c** USEDM, and **d** PM-USEDM, machining parameters: 48 A pulse current and 400-μs pulse duration

ultrasonic vibration of tool and the existence of nanopowder in dielectric simultaneously were more efficient on crack reduction compared with applying them separately. Since each technique had its influence on micro cracks reduction, they intensified each other's effect. For example, the existence of nanopowders in dielectric accompanied with ultrasonic waves affected these particles to move faster and accelerate in plasma channel. Collisions of these accelerated particles with melted layer caused more molten material ejection from each puddle, so the thickness of recast layer had decreased. It had direct effect on crack reduction in machined surface.

3.4 The effects of hybrid EDM processes on the depth of altered metal zone

After EDM process, an altered metal zone had formed on the discharged surface, and it was composed of recast layer and heat affected zone. EDM process changed the metallurgical structure and the characteristics of this region. Micro cracks were formed in this very hard, brittle layer due to the increase in non-homogeneities of metallurgical phases within it. The recast layer was outer layer and was the result of the resolidification of the melted material which was not thrown out from the discharged

region. This layer had high hardness, good adherence to the bulk, and good corrosion resistance. However, the recast layer had increased the surface roughness made the surface hard and brittle and had decreased the fatigue strength due to the presence of micro cracks and microvoids. The SEM images of altered metal zone of different EDM processes are represented in Fig. 8.

The altered metal zones of traditional EDM and PMEDM are presented in Fig. 8a, b. SEM of Fig. 8a was taken at ×500 magnification, while the others were taken at ×2000 magnification. The altered metal zone in traditional EDM was thicker than other processes; its thickness was about four times of the thickness of altered metal zone in PMEDM and USEDM processes. In PMEDM and USEDM processes, the depth of altered zone was reduced significantly. There was a little difference between Fig. 8b, c which belonged to PMEDM and USEDM process, respectively. The effects of nanopowders in dielectric on recast layer (outer part of metal-altered zone) could be explained as follows: the diameter and the length of discharge channel in powder-mixed dielectric were greater than the traditional EDM. In this condition, powder-mixed dielectric fluid produced more electrical discharges that leads to increase in the number of sparks formed in a single pulse,

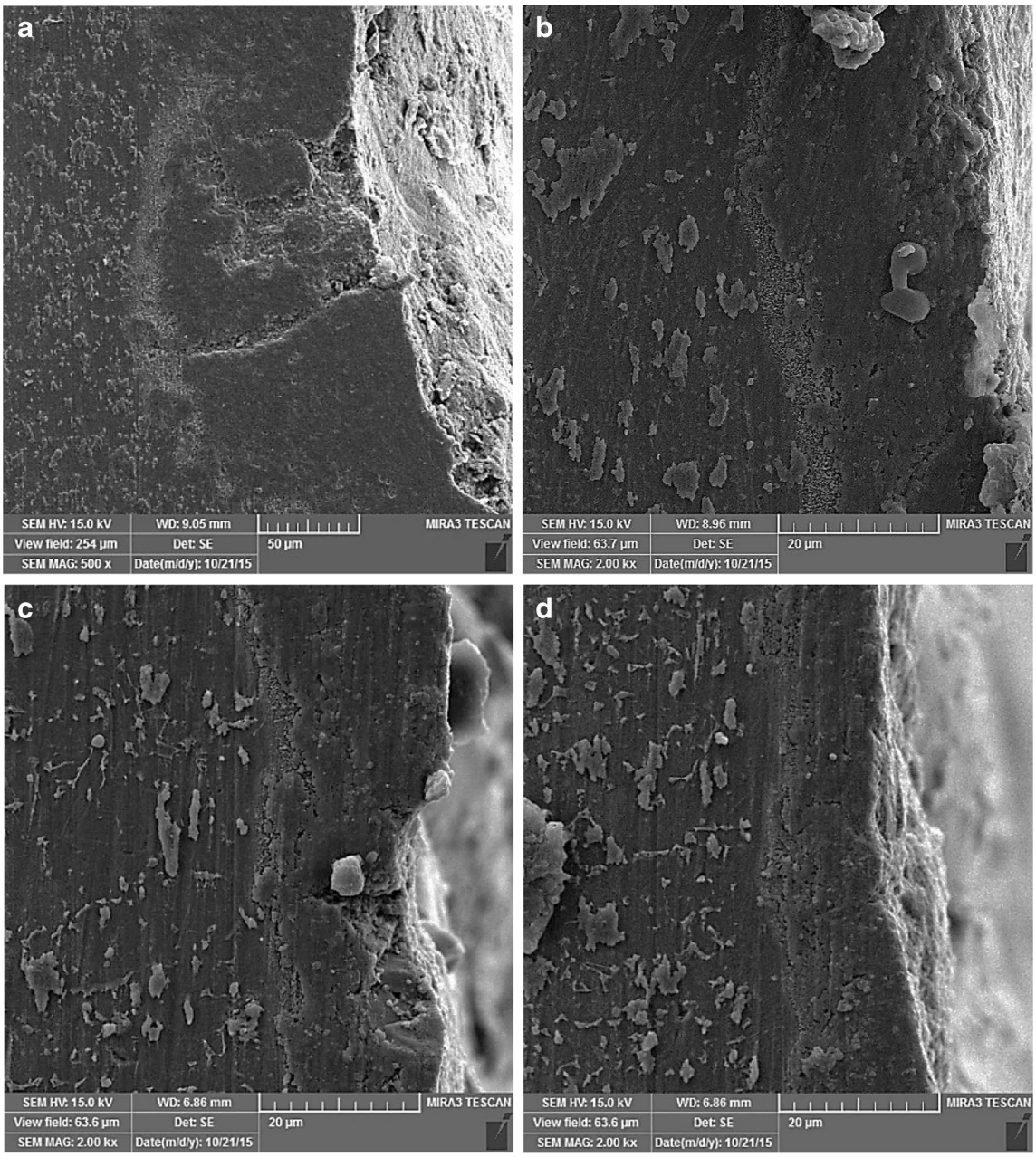

Fig. 8 SEM micrograph of cross section of machined surface in processes **a** EDM, **b** PMEDM, **c** USEDM, and **d** PM-USEDM, machining parameters: 48 A pulse current and 400-µs pulse duration

and discharging energy was dispersed to a larger area, so the depth of melted zone and recast layer was decreased [8].

By adding nanopowders to dielectric, the rate of forming plasma channel and igniting breakdown was faster than the traditional EDM, so there was fewer accumulated energy before the breakdown period, and as a result, thinner altered metal zone was formed in this process [32]. As indicated in Section 3.1, removed melted material in USEDM was more than conventional EDM, so that the recast layer of hybrid USEDM process became thinner [33, 34].

The effects of stimulus ultrasonic vibration of tool and the addition of nanoparticles in dielectric to altered metal zone are shown in Fig. 8d. As it is apparent from this figure, the layer was thinner in comparison to the other machining processes. This case might be described by the reasons declared in Section 3.3. However, it would be worthwhile to state that combination of USEDM technique with nanopowder added dielectric amplified the effects of each other in reducing altered metal zone depth.

3.5 The effects of hybrid EDM processes on residual stress

Residual stress had notable role on surface integrity and fatigue life of sensitive components and structures. In many thermal processes for removing residual stress, posttreatment processes were performed on produced parts. In EDM process, tensile residual stress was developed on machined parts which in many cases affect the proper performance of them.

The results of measuring residual stress of machined workpieces by nanoindentation technique are presented in Fig. 9. Residual stress of machined samples in 100-μs pulse duration and 6, 24, and 48 A pulse current are illustrated in Fig. 9a, b, and c, respectively. As it was demonstrated in these figures, the residual stress curves of hybrid processes in which ultrasonic vibrations were used were similar to each other, and residual stress curves of EDM and PMEDM processes were the same, too.

In all of the residual stress curves, the initial stress value was in a determined amount, but its value was maximized as

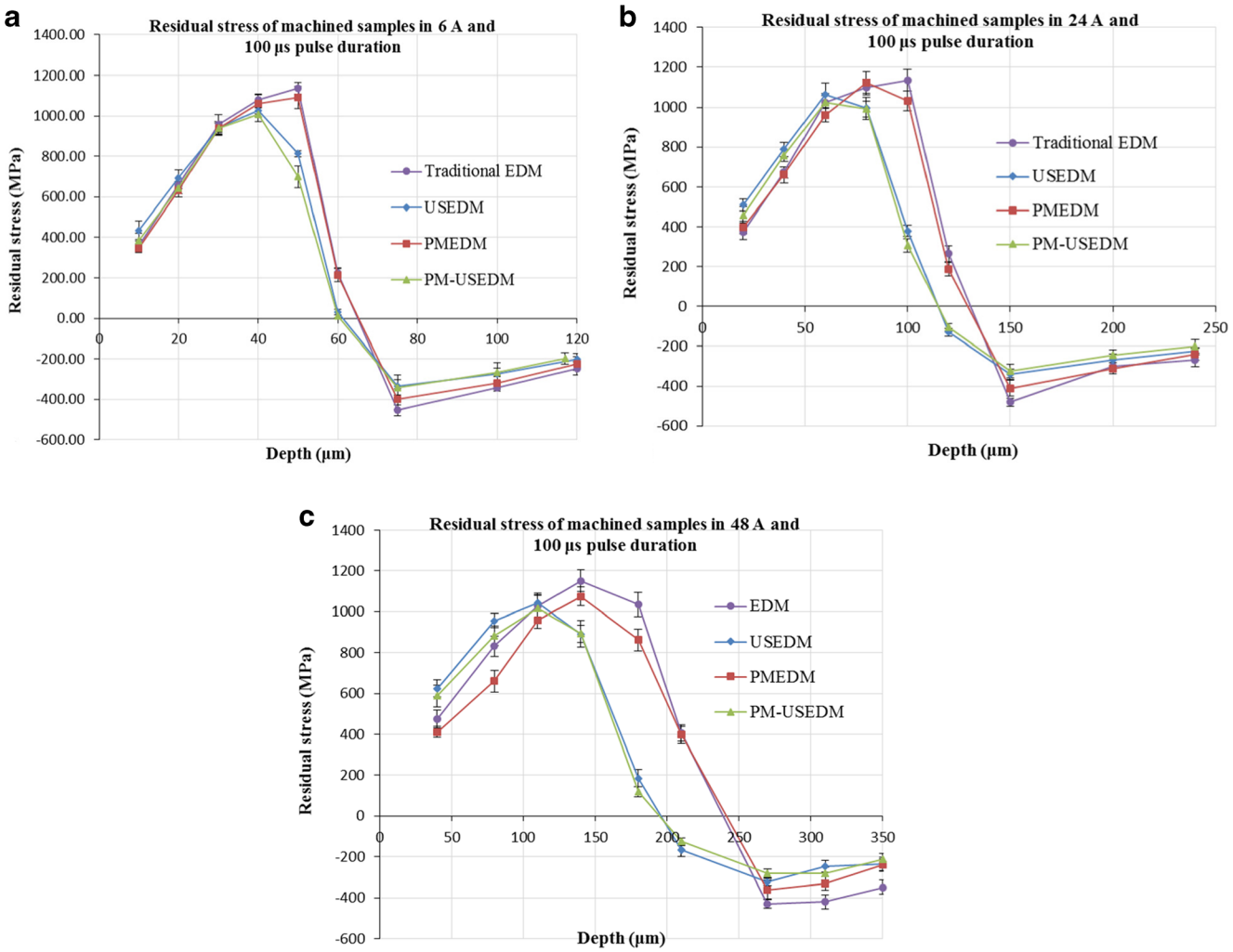

Fig. 9 Residual stress of machined workpieces by different hybrid EDM in **a** 6 A pulse current and 100-μs pulse duration, **b** 24 A pulse current and 100-μs pulse duration, **c** 48 A pulse current, and 100-μs pulse duration

the depth of it increased. Thereafter, this amount had rapidly decreased and had changed to compressive residual stress; finally, it was settled to zero value because of its self-equilibrium characteristic [34]. However, the minimum value that the stresses began in that value, the expected depth of maximum value, and finally, the depth of conversion to compressive stresses and disappearance were all different in various hybrid processes and machining setting.

It would be expressed that when the pulse current increases, the differences between the processes that were conducted by the aid of ultrasonic vibration were more distinct than the other methods. In addition, in the beginning of all curves, the residual stress of ultrasonic-assisted process was greater than the others, but the maximum amount of it was lower, and in smaller depth, it was changed to compressive state. In this manner, without considering their sign, their compressive stresses were smaller. The differences between the curves were analyzed as follows:

In PMEDM process, a discharge was converted to some smaller discharges; in this case, there were not any considerable change in remained melted material on the workpiece surface. But the peak residual stress in ultrasonic-assisted processes was lower compared other processes. In ultrasonic-assisted processes, considering the mechanisms described in Section 3.1, the presence of elastic waves caused more melted materials ejection from molten puddles; consequently, the volume of recasted material was decreased, and the peak residual stresses were reduced due to solidification of the thinner layer.

The reasons for higher residual stresses of ultrasonic-assisted process at the beginning of charts could be clarified as follows: the presence of more and bigger micro cracks of traditional EDM and PMEDM released some amount of residual stresses. As shown in Fig. 7, micro cracks of ultrasonic-assisted process were lower in comparison to the other processes. Therefore, the appearance of cracks in traditional EDM and PMEDM reduced to the near surface residual stresses in these processes.

As it is obvious in Fig. 9a, b, and c by increasing pulse current, the residual stresses of different processes were extended to greater depth. It was due to increase in input energy to the workpiece as a result of higher pulse current that left more molten material in the cavity and consequently the depth of the recasted layer increased so residual stresses extended to the greater depth from the surface of the workpiece.

4 Conclusion

In this research, USEDM, PMEDM, and US-PMEDM processes were used for machining of Ti-6Al-4V titanium alloy. The effects of these techniques on surface integrity and residual stress of machined parts were evaluated and were compared with traditional EDM. The final results of this work were summarizes as follows:

- MRR of hybrid processes was higher than the traditional EDM (MRR ratio >1). In this case, the effect of applying ultrasonic vibration on MRR ratio was more than adding Nanopowders into dielectric and the combination of these hybrid processes had the greatest influence on MRR ratio increase.
- Applying ultrasonic vibration increased surface roughness of machined specimens; the lowest surface roughness among the mentioned hybrid processes belonged to PMEDM process.
- The traditional EDM process developed wider and greater cracks on machined surface; in ultrasonic-assisted and nanopowder-mixed dielectric processes, the length and the width of cracks had been decreased. Surface quality in terms of surface cracks was very favorable in PM-USEDM process.
- The altered metal zone of traditional EDM was very deeper than the other processes. In PMEDM and USEDM processes, the depth of altered zone was reduced significantly. There was a little difference between altered metal zone of PMEDM and USEDM processes. The thinnest altered metal zone belonged to PM-USEDM process.
- Residual stress curves of USEDM and PM-USEDM processes were resembled to each other, and residual stress curves of EDM and PMEDM processes were very similar. In all processes, residual stress initial value was a certain amount that its value was maximized by increasing its depth. Then, it was decreased rapidly and was changed to compressive residual stress and finally was settled to zero value. The first and maximum point of residual stress curve and the depth, in which the residual stress converted to compressive state, were different in various hybrid processes and machining setting.
- Near surface residual stress of ultrasonic-assisted process was greater than the others, but the maximum amount of this was lower, as well, in smaller depth, this stress was changed to compressive state. The results also confirmed that the compressive stresses of this were smaller (without considering the sign of them).

References

1. Yadav V, Jain VK, Dixit PM (2002) Thermal stresses due to electrical discharge machining. Int J Mach Tools Manuf 42:877–888. doi:10.1016/S0890-6955(02)00029-9
2. Shabgard MR, Alenabi H (2015) Ultrasonic assisted electrical discharge machining of Ti–6Al–4V alloy. Mater Manuf Process 30(8): 991–1000. doi:10.1080/10426914.2015.1004686
3. Dibitonto D, Eubank T, Patel MR, Barrufet MA (1989) Theoretical models of the electrical discharge machining process. I. A simple cathode erosion model. J Appl Phys 66:4095–4103. doi:10.1063/1.343994

4. Mamalis AG, Vosniakos GC, Vaxevanidis NM (1987) Macroscopic and microscopic phenomena of electro-discharge machined steel surfaces: an experimental investigation. J Mech Work Technol 15: 335–356. doi:10.1016/0378-3804(87)90047-7
5. Lim LC, Lee LC, Wong YS, Lu HH (1991) Solidification microstructure of electro discharge machined surfaces of tool steels. Mater Sci Technol 7:239–249. doi:10.1179/026708391790183411
6. Sidhom H, Ghanem F, Amadou T, Gonzalez G, Braham C (2013) Effect of electro discharge machining (EDM) on the AISI316L SS white layer microstructure and corrosion resistance. Int J Adv Manuf Technol 65:141–153. doi:10.1007/s00170-012-4156-6
7. Biswas CK, Pradhan MK (2012) FEM of residual stress of EDMed surfaces. Adv Mater Res 383-390:872–876. doi:10.4028/www.scientific.net/AMR.383-390.872
8. Kremer D, Lebrun JL, Hosari B, Moisan A (1989) Effects of ultrasonic vibrations on the performances in EDM. Ann ClRP 38:199–202. doi:10.1016/S0007-8506(07)62684-5
9. Ekmekci B, Tekkaya AE, Erden A (2006) A semi-empirical approach for residual stresses in electric discharge machining (EDM). Int J Mach Tool Manuf 46:858–868. doi:10.1016/j.ijmachtools.2005.07.020
10. Mamalis G, Vosniakos GC, Vacevanidis NM (1988) Residual stress distribution and structural phenomena of high-strength steel surfaces due to EDM and ball-drop forming. Ann CIRP 37(1):531–535. doi:10.1016/S0007-8506(07)61694-1
11. Das S, Klotz M, Klocke F (2003) EDM simulation: finite element-based calculation of deformation, microstructure and residual stresses. J Mater Process Technol 142:434–451. doi:10.1016/S0924-0136(03)00624-1
12. Guu YH, Hocheng H, Chou CY, Deng CS (2003) Effect of electrical discharge machining on surface characteristics and machining damage of AISI D2 tool steel. Mater Sci Eng A358:37–43. doi:10.1016/S0921-5093(03)00272-7
13. Ghanem F, Braham C, Fitzpatrick ME, Sidhom H (2002) Effect of near-surface residual stress and microstructure modification from machining on the fatigue endurance of a tool steel. J Mater Eng Perform 11(6):631–639
14. Ghanem F, Fredj NB, Sidhom H, Braham C (2011) Effects of finishing processes on the fatigue life improvements of electro-machined surfaces of tool steel. Int J Adv Manuf Technol 52: 583–595. doi:10.1007/s00170-010-2751-y
15. Casas B, Torres Y, Llanes L (2006) Fracture and fatigue behavior of electrical-discharge machined cemented carbides. Int J Refract Met Hard Mater 24:162–167. doi:10.1016/j.ijrmhm.2005.04.007
16. Rebelo JC, Dias AM, Kremer D, Lebrun JL (1998) Influence of EDM pulse energy on the surface integrity of martensitic steels. J Mater Process Technol 84:90–96. doi:10.1016/S0924-0136(98)00082-X
17. Yang X, Han X, Zhou F, Kunieda M (2013) Molecular dynamics simulation of residual stress generated in EDM. Procedia CIRP 6: 433–438. doi:10.1016/j.procir.2013.03.037
18. Lütjering G, Williams JC (2007) Titanium, 2nd edition, Springer, Verlag-Berlin Heidelberg
19. Matthew J, Donachie Jr (2000) Titanium: a technical guide, 2nd edn, ASM International
20. Zhu LN, Xu BS, Wang HD, Wang CB (2010) Measurement of residual stress in quenched 1045 steel by the nanoindentation method. Mater Charact 61:1359–1362. doi:10.1016/j.matchar.2010.09.006
21. Anthony C, Cripps F (2011) Nanoindentation, Third Edition, Springer-Verlag New York
22. Lee YH, Kwon D (2004) Estimation of biaxial surface stress by instrumented indentation with sharp indenters. Acta Mater 52(6): 1555–1563. doi:10.1016/j.actamat.2003.12.006
23. Suresh S, Giannakopoulos AE (1999) A new method for estimating residual stresses by instrumented sharp indentation. Acta Mater 46(16):5755–5767. doi:10.1016/S1359-6454(98)00226-2
24. Murthy VSR, Philip PK (1987) Pulse train analysis in ultrasonic assisted EDM. Int J Mach Tool Manuf 27(4):469–477. doi:10.1016/S0890-6955(87)80019-6
25. Takeshi H, Masanori H, Toshiaki O (2002) Mechanical vibration assisted plasma etching for etch rate and anisotropy improvement. Precis Eng 26(4):442–447. doi:10.1016/S0141-6359(02)00151-4
26. Abdullah A, Shabgard MR (2008) Effect of ultrasonic vibration of tool on electrical discharge machining of cemented tungsten carbide (WC-Co). Int J Adv Manuf Technol 38:1137–1147. doi:10.1007/s00170-007-1168-8
27. Shabgard MR, Kakolvand H, Seyedzavvar M, Shotorbani RM (2011) Ultrasonic assisted EDM: effect of the workpiece vibration in the machining characteristics of FW4 Welded Metal. Front Mech Eng 6(4):419–428. doi:10.1007/s11465-011-0246-7
28. Prihandana GS, Mahardika M, Hamdi M, Wong YS, Mitsui K (2009) Effect of micro-powder suspension and ultrasonic vibration of dielectric fluid in micro-EDM processes-Taguchi approach. Int J Mach Tool Manuf 49:1035–1041. doi:10.1016/j.ijmachtools.2009.06.014
29. Prihandana GS, Mahardika M, Hamdi M, Wong YS, Mitsui K (2011) Accuracy improvement in nanographite powder-suspended dielectric fluid for micro-electrical discharge machining processes. Int J Adv Manuf Technol 56:143–149. doi:10.1007/s00170-011-3152-6
30. Shabgard MR, Khosrozadeh B, Sadizadeh B, Kakoulvand H (2013) Comparative study of the effect of ultrasonic vibration of work piece in the electrical discharge machining (EDM). Modares Mech Eng 13(12):48–55 (in Persian)
31. Kumar H (2015) Development of mirror like surface characteristics using nano powder mixed electric discharge machining (NPMEDM). Int J Adv Manuf Technol 76(1):105–113. doi:10.1007/s00170-014-5965-6
32. Wang Y, Zhao F, Liu Y (2008) Behaviors of suspended powder in powder mixed EDM. Key Eng Mater 375-376:36–41. doi:10.4028/www.scientific.net/KEM.375-376.36
33. Lin YC, Yan BH, Chang YS (2000) Machining characteristics of titanium alloy (Ti-6Al-4V) using a combination process of EDM with USM. J Mater Process Technol 104:171–177. doi:10.1016/S0924-0136(00)00539-2
34. Ekmekci B (2007) Residual stresses and white layer in electric discharge machining (EDM). Appl Surf Sci 253:9234–9240. doi:10.1016/j.apsusc.2007.05.078